Osseointegration and antibacterial effect of an antimicrobial peptide releasing mesoporous titania implant

Received: 17 September 2020 | Revised: 21 December 2020 | Accepted: 22 February 2021

DOI: 10.1002/jbm.b.34838

RESEARCH ARTICLE

Society For Biomaterials | WILEY

Osseointegration and antibacterial effect of an antimicrobial peptide releasing mesoporous titania implant

Maria Pihl[1] | Silvia Galli[2] | Ryo Jimbo[2] | Martin Andersson[1]

[1]Department of Chemistry and Chemical Engineering, Applied Chemistry, Chalmers University of Technology, Göteborg, Sweden

[2]Department of Prosthodontics, Faculty of Odontology, Malmö University, Malmö, Sweden

Correspondence
Martin Andersson, Department of Chemistry and Chemical Engineering, Applied Chemistry, Chalmers University of Technology, Göteborg, Sweden.
Email: martin.andersson@chalmers.se

Funding information
Knut och Alice Wallenbergs Stiftelse

Abstract

Medical devices such as orthopedic and dental implants may get infected by bacteria, which results in treatment using antibiotics. Since antibiotic resistance is increasing in society there is a need of finding alternative strategies for infection control. One potential strategy is the use of antimicrobial peptides, AMPs. In this study, we investigated the antibiofilm effect of the AMP, RRP9W4N, using a local drug-delivery system based on mesoporous titania covered titanium implants. Biofilm formation was studied in vitro using a safranine biofilm assay and LIVE/DEAD staining. Moreover, we investigated what effect the AMP had on osseointegration of commercially available titanium implants in vivo, using a rabbit tibia model. The results showed a sustained release of AMP with equal or even better antibiofilm properties than the traditionally used antibiotic Cloxacillin. In addition, no negative effects on osseointegration in vivo was observed. These combined results demonstrate the potential of using mesoporous titania as an AMP delivery system and the potential use of the AMP RRP9W4N for infection control of osseointegrating implants.

KEYWORDS
biofilm, rabbit tibia model, *Staphylococcus epidermidis*, sustained release

1 | INTRODUCTION

A majority of orthopedic implant-related infections are caused by the skin bacteria *Staphylococcus epidermidis* and *Staphylococcus aureus*.[1] Despite that *S. epidermidis* has a low level of virulence and usually does not cause severe infections, they give persistent low-level infections that are difficult to treat. The virulence of *S. epidermidis* is connected to its ability to adhere to surfaces and form biofilms,[2] which can be up to 1,000 times more antibiotic resistant than their corresponding planktonic counterparts.[3] Due to their high antibiotic tolerance, alternatives to treat these infections must be found. A potential group of substances to eradicate biofilms are antimicrobial peptides, AMPs. They strike widely against bacteria, fungi, parasites and some viruses by destroying the cell membrane. The initial interaction between AMP and microbe is thought to occur via electrostatic interactions between the positively charged AMP and negatively charged groups on the bacterial membranes, for example, lipopolysaccharides and lipoteichoic acids.[4] This interaction is followed by rupturing of the bacterial membrane resulting in cell death. Although natural existing AMPs suffer from problems such as proteolytic degradation and cytotoxicity, they can be improved by peptide engineering. Then, proteolytically stable antimicrobial peptides with low toxicity for human cells and high bactericidal effect, even against multi-resistant bacterial strains of *S. aureus*, Group A streptococci, *Escherichia coli* and *P. aeruginosa*, can be obtained.[5] Engineered AMPs have also shown antibacterial properties against other bacteria like *Enterococcus faecium*, *S. aureus*, *Klebsiella pneumoniae*, *Acinetobacter baumanii*, *Pseudomonas aeruginosa*, *Enterobacter cloacae and Escherichia coli*.[6,7] In addition to engineering AMPs, their stability and function may also be improved by the mode of delivery.[8]

As an alternative to administering antimicrobials systemically, local drug-delivery systems may be used when fighting biofilms, with benefits including high local concentrations without the risk of systemic toxic concentrations and an unaffected normal bacterial flora at uninfected areas. Some local strategies used are coatings preventing bacterial adhesion or coatings containing or releasing antimicrobials.[9] Local delivery systems of AMPs that have been evalauted include polymer functionalized carriers,[10] calcium phosphate carriers,[11] silica carriers[12] and cubosomes.[13] Titania surfaces can also be modified for local AMP delivery, using for example, covalent grafting of peptides[14] or nanotubes.[15,16] Mesoporous titania is a potential candicate for local delivery of AMPs, since it possess a good drug loading capacity with controlled relase kinetics, which can be altered by changing material properties such as pore size, surface area and surface chemistry.[17] For antimicrobial purposes, mesoporous titania coating has shown to be efficient in releasing antibiotics for elimination of *S. aureus* and *P. aeruginosa*.[17]

In this study, we investigated the antibacterial effect of the PRELP-derived antimicrobial peptide RRPRPRPRPWWWW-NH2 (RRP9W4N) when incorporated into mesoporous titania. RRP9W4N has shown to have good bacterial killing properties combined with low toxicity to bone forming cells, human osteosarcoma MG63 cells, and human mesenchymal stem cells *in vitro*.[18] The loading and release of peptide from mesoporous titania was investigated as was the antibacterial effect, using a *S. epidermidis* biofilm safranine assay together with LIVE/DEAD *Bac*Light staining and confocal laser scanning microscopy. The antimicrobial activity of the AMP was compared to the clinically used antibiotic Cloxacillin. Moreover, the effect of the AMP on the osseointegration process was evaluated *in vivo* using a rabbit tibia model. This was performed to evaluate if the procedure resulted in a selective implant, that is, high antimicrobial effect combined with no negative consequences on the osseointegration. In the *in vivo* study, commercially available dental titanium implants were installed and followed at different healing times.

2 | MATERIALS AND METHODS

2.1 | Formation of mesoporous titania films

Mesoporous titania films were formed on different substrates using the evaporation induced self-assembly method, EISA, as earlier described.[19] The block copolymer Pluronic 123 (Sigma Aldrich) was used as template and titanium(IV)tetraethoxide (Sigma Aldrich) was used as the inorganic precursor. The 0.5 g Pluronic 123 was dissolved in 8.5 g ethanol (99.5%, Solveco) and stirred for 2 hrs using a magnetic stirrer. In a separate vial, 2.1 g of titanium(IV)ethoxide and 1.6 g HCl (37%, Sigma Aldrich) were mixed and stirred for 2 hrs using a magnetic stirrer, before added to the Pluronic solution and stirred overnight. The concentrations used were chosen to form a cubic mesoporous structure.[20]

Mesoporous thin films were formed using spin-coating (Spin 150, SPS-Europe, 7,000 rpm, 60 s) on different substrates: cover glass slides (VWR), QCM-D sensors (Q-sense), titanium discs (Alfa Aesar) and commercially available threaded titanium implants with a diameter of 3.5 mm and a length of 7 mm (Neodent, Curitiba, Brazil). After spin coating, the surfaces were left overnight in room temperature allowing for the self-assembly to complete and the ethanol to evaporate. The thin films were then calcined to remove the Pluronic template and increase titania cross-linking density through condensation. The samples were heated at a rate of 1°C/min to 350°C, and then left to dwell for 4 h before slowly cooled to room temperature. Nonporous thin titania films were prepared using the same procedure, but without addition of Pluronic 123. The implants were immersed in 200 μM AMP for 24 h and air dried before sterilization by gamma-radiation. This procedure gave a film thickness of 200 nm.[19]

2.2 | Surface characterization

Transmission electron microscopy was used to investigate the mesoporous titania. Microscopy specimens were prepared by scraping off mesoporous titania coated glass slides, mortaring and dispersing in ethanol. A drop of the ethanol dispersion was placed on a holey carbon coated copper grid and left to dry before analysis, in a JEOL JEM 1200EX II microscope operated at 120 kV. Surface morphology was examined with scanning electron microscopy using a Leo Ultra 55 FEG *SEM* operated at 4 kV. Before analysis, the samples were sputtered with gold for 30 s. X-ray photoelectron spectroscopy (XPS) analyses were performed on a Quantum 2000 scanning microprobe from Physical Electronics with an Al Kα (1,486.6 eV) X-ray source. The information depth is approximately 4–5 nm. Contact angle measurements were performed on an optical tensiometer Attension Theta instrument.

2.3 | AMP loading and release from mesoporous titania

Titanium sensors (QSX 310, Q-Sense) were coated with mesoporous titania as described above. Non-coated titanium disks were used as reference. The sensors were washed as recommended by the manufacturer. First, sensors were treated in UV/Ozone for 20 min followed by cleaning in 2% sodium dodecyl sulphate (SDS) for 30 min before washing extensively with MilliQ water. Then samples were dried in nitrogen gas before being subjected to UV/Ozone for another 10 min.

The QCM-D experiments were performed on a Q-Sense E4 instrument. Sensors were mounted in the QCM-D chamber and milliQ water (18.2 MΩ) was used to obtain a baseline (25 μl/min, 21°C). Then Cloxacillin sodium salt monohydrate (0.5 g/L, pH 7.5, Sigma Aldrich) or RRP9W4N (200 μM, Biopeptide, 95%) was flowed over the sensors (25 μl/min, 21°C) and allowed to enter the pores of the mesoporous titania. After antimicrobial loading of the pores, (4 h for AMP, 24 h for Cloxacillin) milliQ water was flowed over the sensors to monitor the antimicrobial release.

2.4 | Biofilm formation

Two bacterial strains of *Staphylococcus epidermidis* were used, the fresh isolate Mia[21] and the type strain CCUG 39508 (Culture Collection University of Göteborg). The strains were cultured on Brain heart infusion agar plates at 37°C. Colonies were transferred to 5 ml liquid Todd Hewitt medium and incubated overnight (37°C) before being transferred to 100 ml fresh Todd Hewitt medium and incubated overnight. Then, bacteria were harvested, washed by centrifugation (2,500 rpm, 10 min) and resuspended in fresh Todd Hewitt medium.

Heat-sterilized mesoporous titania samples were submerged into a solution of 0.5 g/L Cloxacillin, pH 7.5 or 200 μM of the antimicrobial peptide RRPRPRPRPWWWW-NH2 (Biopeptide, 95%, RRP9W4N) and left to soak for 24 hrs to incorporate the antimicrobial substances into the mesoporous film.

Freshly prepared *S. epidermidis* cultures (1×10^9 CFU/ml strain Mia, 7×10^8 CFU/ml strain CCUG 39508) were allowed to grow on the antimicrobial soaked surfaces. Mesoporous titania coated discs without antimicrobials were used as controls.

Bacteria were cultured for 24 hrs (37°C) to allow biofilm adherence and then media was discarded, fresh media was added, and biofilm formation was allowed for another 24 hrs (37°C).

2.5 | Biofilm safranine assay

To assess the amount of biofilm formed on the mesoporous titania samples, surfaces of the samples after bacterial culture were stained with safranine. Each surface was rinsed in 2*0.5 ml MilliQ water and the biofilms were fixed with 0.5 ml methanol for 10 min. Surfaces were allowed to air dry before stained with 1 ml 0.1% safranine O (Alfa Aeser) for 10 min and then rinsed with 4*1 ml MilliQ water. The samples were air-dried and safranine was solubilized for 10 min in 95% ethanol. The solutions were collected, and absorbance was recorded with UV–Vis spectroscopy (HP8453, Hewlett Packard) at 532 nm.

2.6 | Biofilm viability

To assess the bacterial viability, biofilms were stained with LIVE/DEAD *Bac*Light (Molecular probes, kit 7007). Samples were washed twice in MilliQ water, and then stained by 4 μl of *Bac*Light (2.5 μl of sample A, 0.5 μl of sample B in 1 ml 0.85% NaCl) and left in the dark for at least 15 min before studied with confocal microscopy using a LSM 700 inverted confocal laser scanning microscope (Zeiss). Light emitted below 555 nm was collected for propidium iodide and light emitted above 560 nm was collected from Syto 9. In each experiment, images covering a total of 1 mm^2 were obtained using the tile scan function and the surface area coverage of live and dead bacteria were measured using the software Volocity.

2.7 | *In vivo* study

To assess the effect of the antimicrobial peptide (RRP9W4N) on osseointegration and bone healing an *in vivo* study in rabbit tibia was performed. Screw shaped titanium implants coated with a thin mesoporous titania film were used as controls and the same implants loaded with AMP were used as tests.

Ethical approval was received by the ethical committee for animal trials of the French Ministry of Education and Research. Thirty New Zealand White rabbits (*Oryctolagus cuniculus)* were used for this animal trial at the Ecole Nationelle Veterinaire D´Alfort, Mason Alfort, France. The animals were anesthetized with general anesthesia with an intravenous dose of medetomidine, 250 μl/kg (Domitor, Zoetis, France), ketamine, 20 mg/kg (Imalgène 1,000, Merial, Sanofi, France) and diazepam, 1 mg/kg (Valium, Roche, France). In addition, local anesthesia with Xylocain was administered in the rabbit tibia. A full-thickness periosteal flap was elevated on the medial tibia plate and the bone was exposed. A sequence of cylindrical drills under irrigation of sterile saline was used to create one osteotomy on each tibia. One test (AMP-loaded) or one control implant (native mesoporous titania) was inserted in each tibia of the rabbits. Then, the flap was sutured with resorbable Vycril (3.0). The rabbits were supplied with analgesic in the form of buprenorphine (Buprécare, Animalcare, UK), and meloxicam (Metacam, Boehringer Ingelheim Vetmedica, Inc., United States) and with a patch of fentanyl (Duragesic, Janssen Pharmaceutica, Beerse, Belgium) for 5 days after surgery. The animals received oral antibiotics (enrofloxacine, 200 mg/L, Baytril, Bayer Animal Health, Germany) for 5 days.

The animals were left to heal in separate cages for 2, 4 or 12 weeks after the surgery. At each healing time, 10 rabbits were euthanized with a lethal injection of sodium pentobarbital (Euthasol, Virbac, Fort Worth). At the re-entries, the rabbit tibia was dissected, and bone-implant blocks were harvested and fixed in 4% paraformaldehyde. Subsequently, the bone-implant samples were dehydrated in ascending concentrations of ethanol and then infiltrated with liquid resin (Technovit 7,200, VLC; Hereaeus Kulzer, Wehrheim, Germany). The samples were embedded in resin through polymerization under UV-light for 4 h.

Histological sections of 40 μm thickness were prepared along the implant longitudinal axis by cutting-grinding technique *ad modum*[22] and they were stained with Toluidine Blue – Pyronin G dye and then analyzed with optical microscopy using an Eclipse ME600 microscope (Nikon, Tokyo, Japan). Histomorphometrical parameters were recorded for each section and included "Bone-to-Implant Contact" (BIC%), described as the percentage of the implant surface which is in direct contact with bone, and "New Bone Area" (NBA%), which is the percentage of new bone that is found within the threads of the implant. Image J software (National Institute for Health, Bethesda, MD) was used for the histomorphometrical measurements as performed on pictures of the histological slides taken with a digital camera (DS-Ri2, Nikon, Japan) connected to the microscope at a magnification between 200× to 400×.

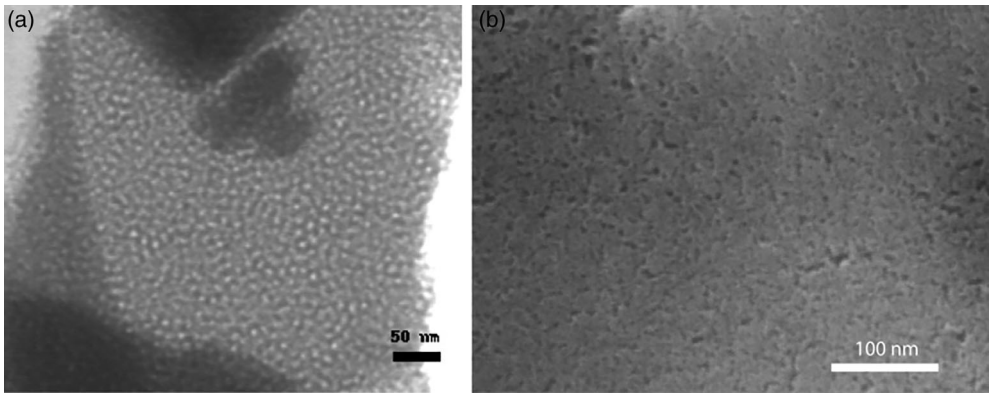

FIGURE 1 Images of mesoporous titania from (a) TEM, scale bar 50 nm and (b) *SEM*, scale bar 100 nm show a porous network with pores extending to the surface

TABLE 1 Contact angles for mesoporous titania and mesoporous titania loaded with antimicrobials

Sample	Contact angle
$MpTiO_2$	21.5 ± 1.8
$MpTiO_2$ RRP9W4N	30.0 ± 1.9
$MpTiO_2$ Cloxacillin	15.6 ± 2.6

2.8 | Statistics

Statistical analysis of the *in vitro* results was performed using one-way ANOVA or Kruskal-Wallis tests and $p < 0.05$ was considered statistically significant. Data are presented as mean ± SD.

In the *in vivo* study, the histomorphometrical results of test and control implants at the different healing times were compared using the non-parametric Wilcoxon Signed Rank test for depended samples and the test and control implants on the same animal were considered as a pair. The analysis was performed with SPSS software (IBM, Version 23.0). Data are presented as mean ± SD.

3 | RESULTS

3.1 | Material characterization

The mesoporous titania was characterized using electron microscopy. In TEM it was clearly observed that the titania consisted of a continuous mesoporous network with pore-diameter of 6 nm, see micrograph in Figure 1(a). The surface of the mesoporous network was examined using *SEM* and pores present on its surface could be seen, Figure 1(b). This indicate the possibility of loading antimicrobial substances into the mesoporous titania.

The water wettability was examined using contact angle measurements and is was shown that the mesoporous titania surfaces were hydrophilic, as can be seen in Table 1. After loading the mesoporous network with either AMP or Cloxacillin, the contact angles changed, indicating the presence of antimicrobials on the surface.

To confirm the presence of antimicrobials, XPS was performed. According to XPS, pure mesoporous titania has a surface composition of about 18% C, 59% O and 23% Ti, whereas the AMP loaded sample had a considerable amount of nitrogen (14% of the sample). Also, the cloxacillin loaded sample contained nitrogen, as well as chlorine, as expected from the compositions of the antimicrobial (Table 2). In addition, some salts were also found on the AMP loaded sample.

3.2 | Drug loading and release

To investigate how much antimicrobials that were loaded into the mesoporous titania, QCM-D experiments were performed see Figure 2. When RRP9W4N was added to the mesoporous titania an immediate, substantial loading of the mesopores could be observed (500 ng/cm^2 within the first 30 min) and maximum loading, 650 ng/cm^2, was reached already after 2.5 hrs. Upon rinsing, there was a slow release of AMP from the surface, continuing until the experiment was aborted at 20 hrs. Then 534 ng/cm^2 of the AMP remained in the mesopores. This is similar to the amount present after initial loading and indicates a very slow release of AMPs. On non-porous titania, RRP9W4N immediately adsorbed and reached its maximum amount of around 180 ng/cm^2 in 2 hrs. This indicates the amount of RRP9W4N that can be loaded into the mesopores is around 470 ng/cm^2. For comparison, the loading of Cloxacillin started with an instant high absorption and then slowly increased for a day (420 ng/cm^2) until rinsing was initiated. That induced an initial burst release followed by a continuous slow release. On non-porous titania, only a small amount of Cloxacillin adsorbed (30 ng/cm^2).

3.3 | Biofilm formation

When using the safranine assay to investigate the biofilm content (Figure 3) there was significantly less ($p < 0.05$) biofilm formation on the mesoporous surfaces loaded with antimicrobials compared to the control mesoporous surface. Furthermore, in one strain (Mia), there was less biofilm on the AMP loaded surface than on the Cloxacillin loaded surface, whereas there was no difference between the antimicrobials for strain 39508.

Biofilm growth and bacterial viability were also investigated using LIVE/DEAD staining and confocal microscopy. The total biofilm

TABLE 2 The XPS results showed that nitrogen was present on the mesoporous titania loaded with AMP or Cloxacillin

	C1s	O1s	Ti2p	N1s	F1s	S2p	Cl2p
$MpTiO_2$	17.7	59.0	23.3				
$MpTiO_2$ RRP9W4N	43.5	32.5	8.7	13.9	1.2	0.2	
$MpTiO_2$ Cloxacillin	26.4	53.4	18.3	1.7			0.3

Abbreviation: XPS, X-ray photoelectron spectroscopy.

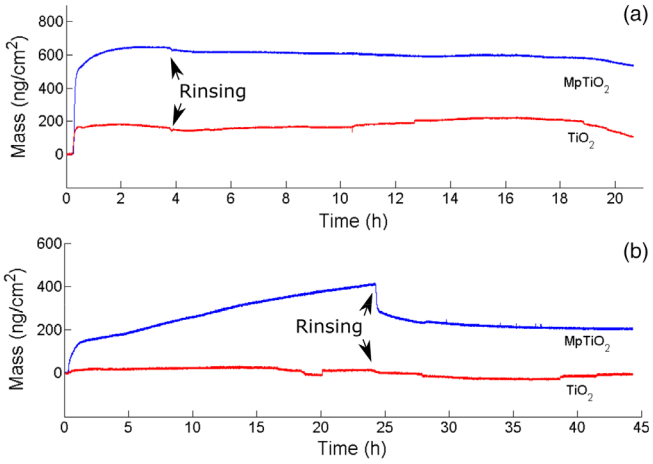

FIGURE 2 (a) Loading of AMP, and (b) Cloxacillin, pH 7.5 into mesoporous titania ($MpTiO_2$). Non-porous titania discs were used as controls (TiO_2)

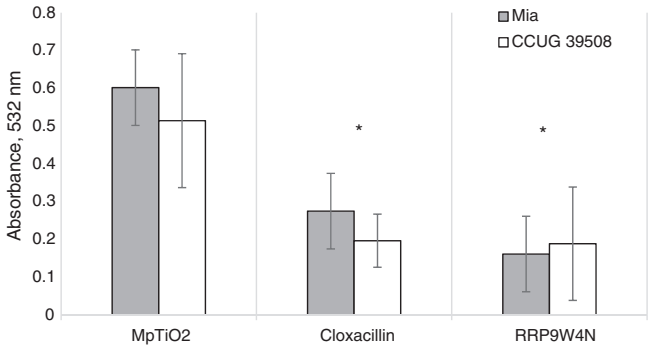

FIGURE 3 The mean biofilm amount (±*SD*) on different surfaces was assessed using safranine staining and statistical significance was calculated using a one way ANOVA test, $p < 0.05$. For both strains the amount of biofilm on the control mesoporous titania surface was statistically significantly higher (*) compared to the Cloxacillin and AMP loaded mesoporous titania

coverage on mesoporous titania and non-porous titania were statistically significant from growth on antimicrobial loaded mesoporous titania, as seen in Figure 4. There was no difference between the antibiotic Cloxacillin and the antimicrobial peptide RRP9W4N. The amount of biofilm eliminated on the two antimicrobial surfaces was 91–94% of the control biofilm on the mesoporous titania, and most bacteria remaining on the samples were alive. In strain Mia, 86–99% of the bacteria were alive whereas in strain 39508, 97–99% of the bacteria were alive.

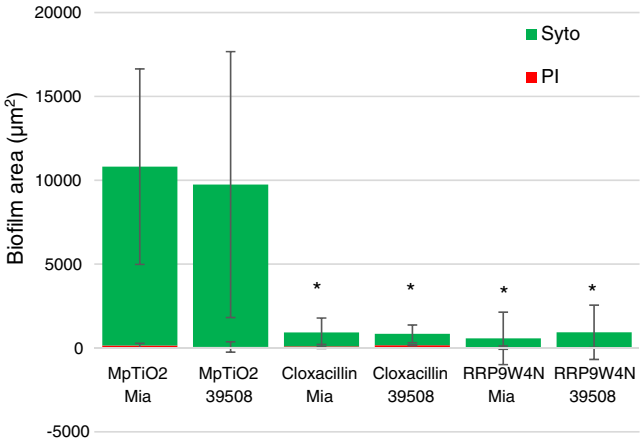

FIGURE 4 The mean (± *SD*) biofilm surface coverage was assessed using *Bac*Light LIVE/DEAD staining and confocal microscopy. Using a Kruskal Wallis test statistical significance could be shown between $MpTiO_2$ compared to Cloxacillin and AMP ($p < 0.01$)

3.4 | *In vivo* results

One rabbit allocated to 2 weeks of healing died during surgery, probably due to complications of the anesthesia. All other animals recovered well from surgery and could walk normally during the follow up period. One sample in the 4-week group was fractured during explantation and three samples, 1 of the 2-week group and 2 of the 12-week group were lost during histological processing. Consequently, the contro-lateral samples in the same animals were removed from analysis, because they could no longer be considered a pair. As a result, a total of eight pairs were included in the analyses at 2 and 12 weeks of healing and a total of nine pairs were included in the analyses at 4 weeks. A power analysis revealed that the sample size obtained was sufficient to detect an effect of the surface treatment on the histomorphometrical parameters. Representative histological images of the test and controls samples are displayed in Figure 5.

After 2 weeks of healing, the original cortical bone was still in contact with the tips of the implant threads, formation of new bone had occurred in the space inside the threads, starting both from the surfaces of the osteotomy and on the implant surfaces. This new bone was organized in thin trabeculae, intensely stained with Toluidine blue and with large osteocyte lacunae and it was extended in the marrow area of the implant as well. No qualitative difference could be observed between the test and the control group. The BIC% was more than twice as high in the test group compared to the control group (8.17% vs 3.46% for the test and control group respectively),

but the difference did not reach a statistical level of significance (p = 0.05). The BA% values were comparable for the test and control implants (24.25% for the test group and 23.21 for the control group).

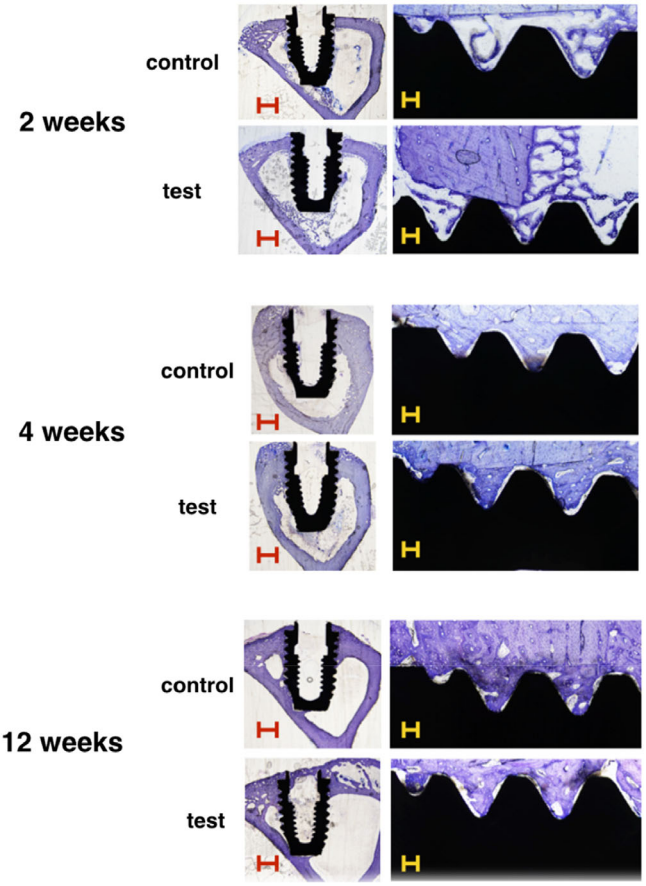

FIGURE 5 Representative toluidine blue stained histological images of the control (no AMP) and test (with AMP) implants at 2, 4 and 12 weeks of healing. Red scale bar: 1000 μm. Yellow scale bar: 100 μm

At week 4 of healing, the new bone had matured and formed a compact and lamellar bone in intimate contact with the implant surface and filling the threads in the cortical region of the tibia. Again, no qualitative differences were observed in the bone maturation between the test and the control groups. The histomorphometrical values were significantly increased from the 2-week observations and were comparable for the test and control samples (BIC%: 16.27% and 21.23% for the test and control group respectively; BA%: 64.60 and 60.50% for the test and control group respectively). Further bone maturation was observed after 12 weeks of healing and the implants were all surrounded by compact and lamellar bone, which extended also in the marrow region, encapsulating large areas of the implants. The average BIC% was 21.46% for the tests and 22.46% for the controls, while the mean BA% was 54.66% for the tests and 52.98% for the controls. The histomorphometrical parameters are reported in Table 3 and Figure 6.

4 | DISCUSSION

In this study, we wanted to investigate the antimicrobial behavior of an engineered AMP, RRP9W4N, in addition to investigating its effect on osseointegration, using commercially available implants coated with AMP loaded mesoporous titania. This was accomplished using both *in vitro* and *in vivo* studies, showing a greatly reduced *in vitro* biofilm formation on mesoporous titania loaded with the AMP and no negative effects on osseointegration *in vivo*.

The rabbit *in vivo* study showed that release of the AMP from the mesoporous titania coated implants did not cause any sign of cellular or tissue toxicity in the proximity of the implants and did not interfere with bone healing and osseointegration of the implants. This is in agreement with our earlier *in vitro* results, showing this AMP, when covalently surface-immobilized, have no toxic effects on mammalian cells.[18] In native form however, AMPs may be toxic to eukaryotic cells, although cytotoxicity often decreases in plasma due to binding of plasma proteins.[23] Due to their endogenous origin, AMPs also

TABLE 3 Histomorphometrical results of the test and control groups 2, 4 and 12 weeks after implant placement. *SD*: standard deviation; Max: maximum value; Min: minimum value. *p*-value was calculated using Wilcoxon Signed Rank for dependent samples

		2 weeks		4 weeks		12 weeks	
		Control	Test	Control	Test	Control	Test
BIC%	Mean	3.46	8.17	21.23	16.27	22.46	21.46
	SD	3.49	7.04	8.49	4.94	10.08	8.61
	Max	11.04	20.04	30.60	23.31	44.93	34.60
	Min	.31	.24	7.27	6.85	11.63	8.60
	Count	8	8	9	9	8	8
	p-value	*.07*		*0.09*		*0.48*	
BA%	Mean	23.21	24.25	60.50	64.60	52.98	54.66
	SD	8.90	12.42	8.96	8.23	13.59	18.45
	Max	34.45	42.59	71.06	76.80	70.33	87.10
	Min	12.06	10.44	43.47	51.92	37.38	29.53
	Count	8	8	9	9	8	8
	p-value	*.78*		*0.26*		*0.57*	

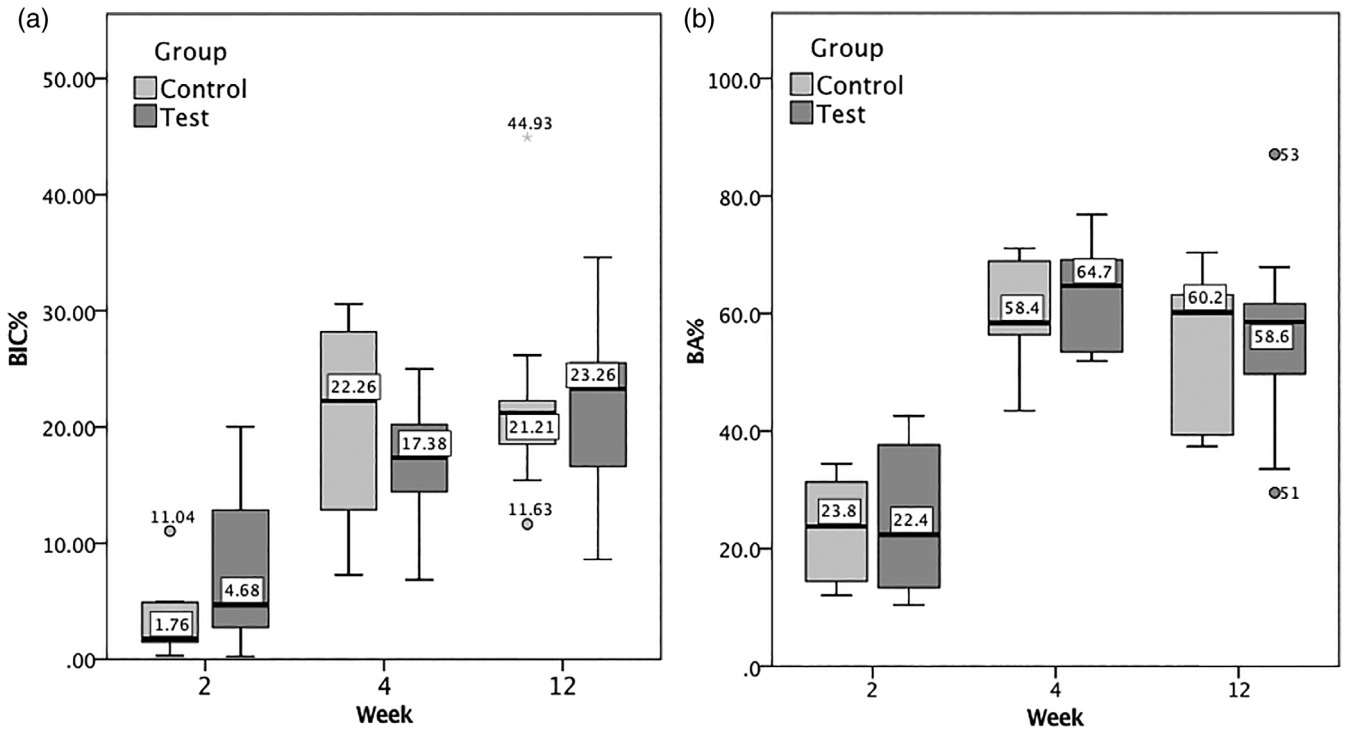

FIGURE 6 Graph showing BIC% (a) and BA% (b) parameters at the different healing stages. The box-plots represent the distribution of the data. The mid-lines of the bars and the values represent the median values

suffer from proteolytic degradation in the body. However, end-tagging of the peptides with the bulky, aromatic amino acids like tryptophan or phenylalanine prevent the peptides from binding eukaryotic cholesterol-containing membranes, resulting in decreased cytotoxicity[24] and by varying the end-tag length proteolytic stability can be achieved.[5] The AMP used in this study, RRP9W4N, has been engineered according to these measures and the *in vivo* results showed the AMP-releasing implants performed in a manner comparable to the control implants with identical surface, but without addition of AMP. In addition, the BIC% was more than twice as high for the test implants than for the control implants after 2 weeks of healing. Despite the difference was not statistically significant, this AMP might have a mild enhancing effect in initial osseointegration. Mild, non-significant, enhancing osseointegrative effects have also been shown for other AMPs.[11] However, more studies need to be performed to make the statement that these AMPs improves the early stages of osseointegration.

In addition to chemically engineered AMPs, their stability and function may also be improved by mode of delivery.[8] For example, elastases from *Pseudomonas aeruginosa* and human neutrophils degrades pure AMP LL-37, but when loaded in cubosomes it can be protected against proteolytic degradation.[13] In this study, mesoporous titania coatings were used and electron microscopy showed a porous network extending to the surface, into which antimicrobials were loaded. The cubic mesoporous network had pore diameters of 6 nm, well above the size of both antimicrobials used, Cloxacillin and RRP9W4N. As has been previously shown using different sized dendrimers, the absorption into mesoporous films is dependent on both pore size and morphology (cubic or hexagonal) where a cubic arrangement results in an increased absorption rate.[25] The cubic mesoporous titania used in the present study clearly facilitate AMP loading into the pores; however, the pore size is small enough to prevent entry of most proteolytic enzymes and other proteins, and thus the mesoporous titania may not only act as a drug carrier but also provide some means of physical protection against proteolytic degradation and other protein interactions that may interfere with the antimicrobial activity. For example, mesoporous silica have shown to prevent proteolytic degradation of a green fluorescent protein.[26] In the *in vitro* studies, rich growth medium was used, meaning a plethora of proteins (although denatured in the autoclave) were present during both culturing and bacterial elimination. Despite this, the AMP was as good a biofilm eliminator as Cloxacillin, indicating the AMP ability to maintain its function despite potential protein binding. This is probably due to its engineered properties to increase its proteolytic stability and the potential of physical protection of the AMPs inside the mesopores.

The QCM-D results showed an immediate, substantial loading of RRP9W4N into the pores and maximum charging was reached already after 2.5 hrs. Upon rinsing, there was a slow release of the peptide, continuing for 20 hrs until the experiment was aborted. At this point of time, only 18% of the total amount of absorbed AMP was released, indicating there is potential for a sustained release antimicrobial surface. The results are in good agreement with the slow release, 17% AMP delivery during the first 24 hrs, that has been shown using mesoporous silica nanoparticles as AMP delivery systems.[27] However,

long time release studies are needed to investigate this further. It should also be emphasized that the drug-release *in vitro* is by no means the same as in the *in vivo* situation, and it is challenging to make direct comparisons. We do not claim that the release kinetics observed here can be directly translated to a clinical situation, but still it gives a good indication that the release is sustained and not delivered in a burst fashion, at least during the first day. In addition to functioning as a drug-delivery system, pure mesoporous titania coatings on implants have also shown a tendency to improve osseointegration *in vivo* compared to non-porous titania.[19]

The major function of AMP is to eliminate microorganisms, and both *in vitro* experiments in this study showed a significantly smaller biofilm on the AMP charged mesoporous surface compared to the non-loaded mesoporous control. The antimicrobial effect of the AMP was comparable or better than what was found for the antibiotic Cloxacillin. Other AMPs, both natural and synthetic, have also shown considerable antibiofilm properties.[28,29] We did not perform any *in vivo* antimicrobial tests, but this AMP has shown an antibacterial effects in human infected blood and in a pig skin wound model *ex vivo*,[5] indicating its potential use in future patient implants. Studying the small proportion of bacteria that were able to adhere to the AMP charged surface, a majority (86–99%) were alive. One hypothesis is that bacteria may adhere to the surface, but a slow, sustained release of AMP efficiently eliminate bacteria in due time and prevent formation of a mature biofilm. We have earlier shown this AMP to initiate swelling and bursting of bacteria on surfaces and complete bacterial eradication, depending on time and concentration.[30]

The results of this study show the combined good *in vitro* bacterial elimination, even in presence of a high initial bacterial load, far larger than what would be found in the clinical setting with no negative effects on *in vivo* osseointegration. We have earlier shown this AMP to be efficient in killing both normal and persister bacteria of *S. epidermidis*, at a concentration of 100–200 μM *in vitro*.[30] This is an important factor in the clinical setting where recurring infections caused by persister cells is a challenging problem.[31] Although the AMP concentration in the mesoporous titania of this study is less, it may be modulated to create an efficient bacterial persister elimination and sustained release of AMP.

5 | CONCLUSION

In this study, the antibacterial effect of the engineered AMP, RRP9W4N on bacterial biofilms, and its influence on osseointegration directly at the implant healing site were examined. The peptide was loaded in mesoporous titania, which was coated into titanium implants. The anti-bacterial property of the AMP was preserved, as demonstrated by the *in vitro* evaluation, while it did not negatively affect osseointegration *in vivo*. The potential benefits of introducing antimicrobial substances into mesoporous titania on implant surfaces is local delivery, facilitating high antimicrobial substance concentration and avoiding systemic side effects. Here, we show the potential of mesoporous titania to deliver antimicrobial peptides in a proteinaceous environment. More than 90% of the biofilms were eliminated *in vitro*, a result equal to that of the clinically used antibiotic Cloxacillin, at the same time as ossoeintegration proceeded without any negative observations. The combined result of this study suggests that AMP loaded mesoporous titania may be a good candidate to lower the risk of implant associated infections.

ACKNOWLEDGEMENTS

We acknowledge the Centre for Cellular Imaging at Sahlgrenska Akademin, Göteborg University for the use of imaging equipment and for the support from the staff. *S. epidermidis* Mia was a kind gift of Professor Gunnel Svensäter, Malmö University. Emma Andersson is thanked for production of mesoporous surfaces used for SEM and TEM. Financial support was received from the Knut och Alice Wallenbergs Stiftelse through their Wallenberg Academy Fellows program.

DATA AVAILABILITY STATEMENT

Data available on request from the authors

REFERENCES

1. Zimmerli W, Moser C. Pathogenesis and treatment concepts of orthopaedic biofilm infections. *FEMS Immunol Med Microbiol*. 2012;*65*(2):158-168. https://doi.org/10.1111/j.1574-695X.2012.00938.x.
2. Vuong C, Otto M. *Staphylococcus epidermidis* infections. *Microbes Infect*. 2002;*4*(4):481-489. https://doi.org/10.1016/s1286-4579(02)01563-0.
3. Hoiby N, Bjarnsholt T, Givskov M, Molin S, Ciofu O. Antibiotic resistance of bacterial biofilms. *Int J Antimicrob Agents*. 2010;*35*(4):322-332. https://doi.org/10.1016/j.ijantimicag.2009.12.011.
4. Jenssen H, Hamill P, Hancock REW. Peptide Antimicrobial Agents. *Clin Microbiol Rev*. 2006;*19*(3):491-511. https://doi.org/10.1128/cmr.00056-05.
5. Malmsten M, Kasetty G, Pasupuleti M, Alenfall J, Schmidtchen A. Highly selective end-tagged antimicrobial peptides derived from PRELP. *PLoS One*. 2011;*6*(1):e16400. https://doi.org/10.1371/journal.pone.0016400.
6. Wang G, Hanke ML, Mishra B, et al. Transformation of human cathelicidin LL-37 into selective, stable, and potent antimicrobial compounds. *ACS Chem Biol*. 2014;*9*(9):1997-2002. https://doi.org/10.1021/cb500475y.
7. Zhang S-K, Song J-W, Gong F, et al. Design of an α-helical antimicrobial peptide with improved cell-selective and potent anti-biofilm activity. *Sci Rep*. 2016;*6*:27394-27394. https://doi.org/10.1038/srep27394.
8. Nordström R, Malmsten M. Delivery systems for antimicrobial peptides. *Adv Colloid Interface Sci*. 2017;*242*:17-34. https://doi.org/10.1016/j.cis.2017.01.005.
9. Zhao L, Chu PK, Zhang Y, Wu Z. Antibacterial coatings on titanium implants. *J Biomed Mater Res B Appl Biomater*. 2009;*91B*(1):470-480. https://doi.org/10.1002/jbm.b.31463.
10. Sun H, Hong Y, Xi Y, Zou Y, Gao J, Du J. Synthesis, self-assembly, and biomedical applications of antimicrobial peptide–polymer conjugates. *Biomacromolecules*. 2018;*19*(6):1701-1720. https://doi.org/10.1021/acs.biomac.8b00208.
11. Kazemzadeh-Narbat M, Noordin S, Fau-Masri BA, et al. Drug release and bone growth studies of antimicrobial peptide-loaded calcium phosphate coating on titanium. *J Biomed Mater Res B Appl Biomater*. 2012;*100*:1344-1352. https://doi.org/10.1002/jbm.b.32701.
12. Izquierdo-Barba I, Vallet-Regí M, Kupferschmidt N, Terasaki O, Schmidtchen A, Malmsten M. Incorporation of antimicrobial

compounds in mesoporous silica film monolith. *Biomaterials*. 2009;*30*(29):5729-5736. https://doi.org/10.1016/j.biomaterials.2009.07.003.
13. Boge L, Umerska A, Matougui N, et al. Cubosomes post-loaded with antimicrobial peptides: characterization, bactericidal effect and proteolytic stability. *Int J Pharm*. 2017;*526*(1):400-412. https://doi.org/10.1016/j.ijpharm.2017.04.082.
14. Chen R, Willcox MD, Ho KK, Smyth D, Kumar N. Antimicrobial peptide melimine coating for titanium and its in vivo antibacterial activity in rodent subcutaneous infection models. *Biomaterials*. 2016;*85*:142-151. https://doi.org/10.1016/j.biomaterials.2016.01.063.
15. Kazemzadeh-Narbat M, Lai BFL, Ding C, Kizhakkedathu JN, Hancock REW, Wang R. Multilayered coating on titanium for controlled release of antimicrobial peptides for the prevention of implant-associated infections. *Biomaterials*. 2013;*34*(24):5969-5977. https://doi.org/10.1016/j.biomaterials.2013.04.036.
16. Li T, Wang N, Chen S, Lu R, Li H, Zhang Z. Antibacterial activity and cytocompatibility of an implant coating consisting of TiO(2) nanotubes combined with a GL13K antimicrobial peptide. *Int J Nanomedicine*. 2017;*12*:2995-3007. https://doi.org/10.2147/IJN.S128775.
17. Atefyekta S, Ercan B, Karlsson J, et al. Antimicrobial performance of mesoporous titania thin films: role of pore size, hydrophobicity, and antibiotic release. *Int J Nanomedicine*. 2016;*11*:977-990. https://doi.org/10.2147/IJN.S95375.
18. Atefyekta S, Pihl M, Lindsay C, Heilshorn SC, Andersson M. Antibiofilm elastin-like polypeptide coatings: functionality, stability, and selectivity. *Acta Biomater*. 2019;*83*:245-256. https://doi.org/10.1016/j.actbio.2018.10.039.
19. Karlsson J, Jimbo R, Fathali HM, et al. In vivo biomechanical stability of osseointegrating mesoporous TiO2 implants. *Acta Biomater*. 2012;*8*(12):4438-4446. https://doi.org/10.1016/j.actbio.2012.07.035.
20. Alberius PCA, Frindell KL, Hayward RC, Kramer EJ, Stucky GD, Chmelka BF. General predictive syntheses of cubic, hexagonal, and lamellar silica and Titania Mesostructured thin films. *Chem Mater*. 2002;*14*(8):3284-3294. https://doi.org/10.1021/cm011209u.
21. Pihl M, Chavez de Paz LE, Schmidtchen A, Svensater G, Davies JR. Effects of clinical isolates of *Pseudomonas aeruginosa* on *Staphylococcus epidermidis* biofilm formation. *FEMS Immunol Med Microbiol*. 2010;*59*(3):504-512. https://doi.org/10.1111/j.1574-695X.2010.00707.x.
22. Donath K. Preparation of histologic sections by cutting-grinding technique for hard tissue and other materials not suitable to be sectioned by routine method. *EXAKT-Kulzer, Norderstedt*. 1993;*1*:16.
23. Johansson J, Gudmundsson GH, Rottenberg MNE, Berndt KD, Agerberth B. Conformation-dependent antibacterial activity of the naturally occurring human peptide LL-37. *J Biol Chem*. 1998;*273*(6):3718-3724. https://doi.org/10.1074/jbc.273.6.3718.
24. Pasupuleti M, Chalupka A, Morgelin M, Schmidtchen A, Malmsten M. Tryptophan end-tagging of antimicrobial peptides for increased potency against *Pseudomonas aeruginosa*. *Biochim Biophys Acta*. 2009;*1790*(8):800-808. https://doi.org/10.1016/j.bbagen.2009.03.029.
25. Claesson M, Ahmadi A, Fathali HM, Andersson M. Improved QCM-D signal-to-noise ratio using mesoporous silica and titania. *Sens Actuators B*. 2012;*166-167*:526-534. https://doi.org/10.1016/j.snb.2012.03.002.
26. Schlipf DM, Rankin SE, Knutson BL. Pore-size dependent protein adsorption and protection from Proteolytic hydrolysis in tailored Mesoporous silica particles. *ACS Appl Mater Interfaces*. 2013;*5*(20):10111-10117. https://doi.org/10.1021/am402754h.
27. Braun K, Pochert A, Lindén M, et al. Membrane interactions of mesoporous silica nanoparticles as carriers of antimicrobial peptides. *J Colloid Interface Sci*. 2016;*475*:161-170. https://doi.org/10.1016/j.jcis.2016.05.002.
28. Rajasekaran G, Kim EY, Shin SY. LL-37-derived membrane-active FK-13 analogs possessing cell selectivity, anti-biofilm activity and synergy with chloramphenicol and anti-inflammatory activity. *Biochimica et Biophysica Acta (BBA) - Biomembranes*. 2017;*1859*(5):722-733. https://doi.org/10.1016/j.bbamem.2017.01.037.
29. Pletzer D, Coleman SR, Hancock RE. Anti-biofilm peptides as a new weapon in antimicrobial warfare. *Curr Opin Microbiol*. 2016;*33*:35-40. https://doi.org/10.1016/j.mib.2016.05.016.
30. Pihl M, Andersson M. *Staphylococcus epidermidis* Persister cell elimination using an antimicrobial peptide. *J Bacteriol Mycol*. 2019;*6*(2):1101. https://doi.org/10.26420/jbacteriolmycol.2019.1101.
31. Lewis K. Persister cells, dormancy and infectious disease. *Nat Rev Microbiol*. 2007;*5*(1):48-56. https://doi.org/10.1038/nrmicro1557.

How to cite this article: Pihl M, Galli S, Jimbo R, Andersson M. Osseointegration and antibacterial effect of an antimicrobial peptide releasing mesoporous titania implant. *J Biomed Mater Res*. 2021;1–9. https://doi.org/10.1002/jbm.b.34838